RSC Sustainability

ROYAL SOCIETY OF CHEMISTRY

PAPER

View Article Online
View Journal | View Issue

Cite this: *RSC Sustainability*, 2025, **3**, 4825

Development of a bio-synthesized zinc oxide nanoparticle sensor for the quantification of totarolone in *Tetraclinis articulata*

Omar anor,[a] Sofia Kerouad, *[a] Issam Forsal,[a] Wissal Kotmani,[a] Mustapha Bouzaid[b] and Latifa Bouissane [cd]

Diterpenoids such as totarolone exhibit significant bioactivity, making their accurate quantification in plant extracts essential for pharmacological studies and quality control. Conventional analytical methods are often time-consuming, costly, or environmentally demanding, highlighting the need for rapid, sensitive, and eco-friendly alternatives. In this work, we report the electrochemical quantification of totarolone, a bioactive diterpenoid, in *Tetraclinis articulata* extract using a carbon paste electrode modified with green-synthesized zinc oxide (bio-ZnO) nanoparticles. Bio-ZnO was prepared *via* a plant-mediated route using *Calamintha nepeta* extract, providing a sustainable and eco-friendly alternative to conventional chemical synthesis. XRD analysis revealed that the bio-ZnO nanoparticles possess a hexagonal wurtzite structure with an average crystallite size of ~10 nm. The modified electrode exhibited enhanced sensitivity and stability, enabling the effective detection of totarolone by cyclic voltammetry (CV) and square wave voltammetry (SWV). A linear analytical response was obtained, with a LOD of 1.19 μM, a LOQ of 3.98 μM and a measured concentration of 0.133 mM in the plant extract. These findings highlight the potential of green nanomaterial-based electrochemical sensors for the reliable and sustainable analysis of bioactive compounds.

Received 25th June 2025
Accepted 28th August 2025

DOI: 10.1039/d5su00477b

rsc.li/rscsus

Sustainability spotlight

The detection and quantification of bioactive molecules from medicinal plants are essential for ensuring their safe, effective, and standardized use in pharmaceutical and nutraceutical applications. However, traditional analytical approaches and nanoparticle synthesis methods often rely on toxic chemicals and energy-intensive processes. In this work, we present a sustainable alternative by using *Calamintha nepeta* extract to synthesize ZnO nanoparticles, which are then used to fabricate a sensitive electrochemical sensor for totarolone determination. This green methodology minimizes environmental impact, aligns with the principles of green chemistry, and supports responsible innovation. The study directly contributes to UN SDG 3 (good health and well-being) and SDG 12 (responsible consumption and production) by promoting eco-friendly sensor development and safe natural product analysis.

1. Introduction

Aromatic and medicinal plants have long served as valuable sources of bioactive compounds for traditional remedies and modern pharmacological applications.[1,2] While significant attention has been devoted to widely used species, forest plants, particularly those from the Cupressaceae family, remain comparatively underexplored.[3] Among them, *Tetraclinis articulata*, an evergreen tree native to the Mediterranean region, stands out for its remarkable adaptability to harsh climatic conditions. Traditionally, this species has been widely utilized in herbal medicine for its therapeutic benefits.[4] Scientific studies have confirmed the diverse biological activities of *T. articulata* extracts and essential oils, demonstrating antioxidant, antimicrobial, insecticidal, cytotoxic, and anti-inflammatory properties.[5,6] These findings underscore its potential for various medicinal applications and highlight the need for further exploration of its bioactive constituents.

One such constituent, totarolone, is a naturally occurring diterpenoid that exhibits notable pharmacological activities, such as anti-lymphangiogenic effects, making it a candidate for therapeutic development in cancer research.[7,8] Beyond its medicinal potential, its bioactive nature makes it an interesting subject for green chemistry approaches, where plant-derived molecules are explored as sustainable alternatives to synthetic

[a]*Laboratory of Engineering and Applied Technologies, School of Technology, Beni Mellal, Morocco. E-mail: sofia.kerouad@usms.ac.ma*

[b]*Environmental, Ecological and Agro-Industrial Engineering Laboratory, Faculty of Science and Technologies, Sultan Moulay Slimane University, PB: 523, Beni Mellal, Morocco*

[c]*Molecular Chemistry, Materials and Catalysis Laboratory, Faculty of Sciences and Technologies, Sultan Moulay Slimane University, BP 523, 23000 Beni-Mellal, Morocco*

[d]*Chemicals Process and Applied Materials Team, Polydisciplinary Faculty, Sultan Moulay Slimane University, BP 523, Beni-Mellal, 23000, Morocco*

compounds. Since totarolone's bioactive properties are essential for its therapeutic and medicinal effects, its reliable quantification in natural matrices is essential not only to ensure consistency in medicinal formulations, but also to support quality control and sustainable utilization of plant-based resources.

Conventionally, techniques such as high-performance liquid chromatography (HPLC) are employed for the quantification of plant-derived bioactive compounds. However, these methods are resource-intensive, requiring organic solvents, extensive sample preparation, and energy-consuming instrumentation,[9,10] thus posing challenges from a green chemistry standpoint. As environmental sustainability becomes a priority in analytical science, there is a pressing need for eco-friendly, low-cost, and efficient alternatives. In this context, electrochemical methods have emerged as promising green analytical tools. They offer several advantages, including minimal solvent use, low E-factor and low energy requirements, and rapid analysis times, making them well suited for sustainable phytochemical detection.[11–13] Furthermore, the performance of electrochemical sensors can be significantly enhanced through the use of nanomaterial-based electrode modifiers.[14]

Zinc oxide nanoparticles (ZnO NPs) are particularly attractive in this regard due to their high surface area, catalytic properties, and electrical conductivity.[15,16] However, traditional synthesis routes for ZnO NPs such as chemical reduction, sol–gel, and laser ablation[17] typically involve toxic reagents and hazardous conditions, contradicting the principles of green chemistry.[18] In response to these concerns, there is growing interest in developing green methods including plant extracts that are non-toxic, environmentally friendly, ecological, simple and cost-effective.[19]

This study employs a green synthesis approach to produce ZnO NPs using an aqueous extract of *Calamintha nepeta* leaves. This plant extract, rich in phytochemicals such as saponins, phenols, flavonoids, and tannins, serves as both reducing and stabilizing nanoparticles,[20,21] eliminating the need for hazardous chemicals and energy-intensive steps.

The resulting bio-ZnO nanoparticles were used to modify a carbon paste electrode (CPE), an economical and reusable sensing platform, to enhance its electrochemical performance. The modified electrode was then applied to the electrochemical investigation of totarolone using cyclic voltammetry (CV) for redox behavior assessment[22] and square wave voltammetry (SWV) for precise quantification. SWV, known for its high sensitivity and resolution,[23] enabled rapid and accurate determination of totarolone in *T. articulata* extracts, offering a promising green alternative to conventional chromatographic methods.

This work contributes to the development of sustainable electrochemical sensors by combining green nanotechnology and phytochemical analysis. The proposed platform offers a non-toxic, cost-effective, and environmentally friendly method for the detection of high-value bioactive compounds in plant matrices, aligning with the principles of green chemistry and the United Nations Sustainable Development Goals (SDGs), particularly SDG 3 (good health and well-being), SDG 9 (industry, innovation and infrastructure), and SDG 12 (responsible consumption and production).[24]

2. Experimental

2.1. Reagents

Every chemical utilized was of analytical grade and did not require any additional purification. Zinc chloride ($ZnCl_2$), sodium chloride (NaCl) and graphite were obtained from Sigma Aldrich.

2.2. Apparatus

The surface morphology of the material was examined using a field emission scanning electron microscope (FE-SEM, model FEG 450).

The spectra of ZnO nanoparticles obtained using FT-IR analyses were recorded using a JASCO FT/IR-4600 spectrometer equipped with an ATR accessory. The ATR-FTIR spectra were recorded in the 4000–600 cm^{-1} range with a resolution of 4 cm^{-1} and an accumulation of 16 scans.

2.3. Bio synthesis of ZnO NPs

2.3.1. Preparation of the extract. *Calamintha nepeta* was collected from El Bassatine, Meknes, Morocco, in April. The plant leaves were washed to eliminate dust and dried for 15 days in shade at room temperature (25–27 °C). The dried leaves were crushed into powder using a blender.

A mixture of 10 g of plant powder and 100 mL of distilled water was heated at 100 °C for 15 minutes. The solution was filtered once it had cooled and retained for the synthesis of bio-ZnO nanoparticles.[25]

2.3.2. Synthesis of bio-ZnO NPs. 50 mL of the *Calamintha nepeta* leaf extract was boiled at 60–80 °C. When the temperature reached 70 °C; 5 g of $ZnCl_2$ was added to the extract. The solution was then continuously heated until the mixture transformed into a brownish paste, a sign that zinc chloride had been reduced. The mixture was centrifuged and then dried for 12 hours at 100 °C. The powder obtained was washed several times with distilled water and methanol before being calcined for 3 h at 400 °C.[25]

2.4. Preparation of the bare CPE and modified CPE

Using a mortar and pestle, 0.08 g of bio-ZnO nanoparticles and 0.8 g of graphite powder were manually mixed to create the modified CPE. The aforesaid mixture was then combined with paraffin and mixed for 30 minutes to create a consistently wet paste. The paste was then put into a syringe tube that had a 2 mm internal radius. To establish electrical contact, a copper wire was pushed inside the tube. An identical method was utilized to manufacture an unmodified CPE, without adding ZnO nanoparticles.[26]

2.5. *Tetraclinis articulata* extract preparation

A total of 500 g of *Tetraclinis articulata* sawdust was subjected to continuous extraction in a Soxhlet apparatus for 24 hours. After

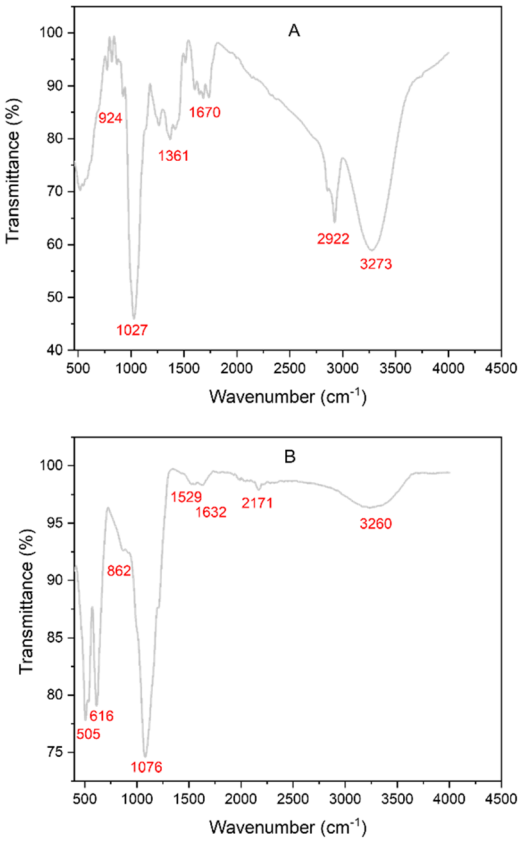

Fig. 1 FTIR spectra of (A) *Calamintha nepeta* extract and (B) bio-synthesized ZnO nanoparticles.

the extraction, the crude residue was recovered by evaporation under reduced pressure. This extract, which contains the bioactive compounds, was stored at 4 °C in the dark for subsequent electrochemical analysis of totarolone content.[27]

2.6. Electrochemical detection protocol

All experiments were conducted using a potentiostat OrigaStat 100 equipped with Origamaster5 software. A conventional three-electrode system was employed, comprising bio-ZnO/CPE as the working electrode, a platinum wire as the counter

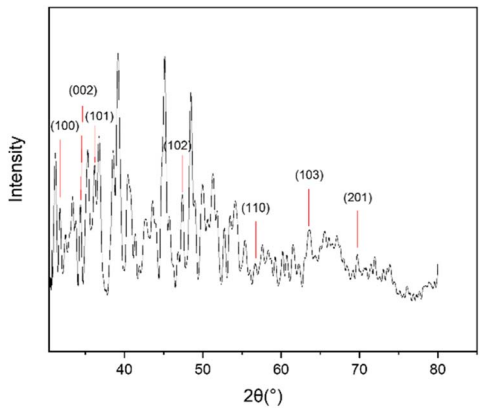

Fig. 2 XRD analysis of bio-synthesized ZnO nanoparticles.

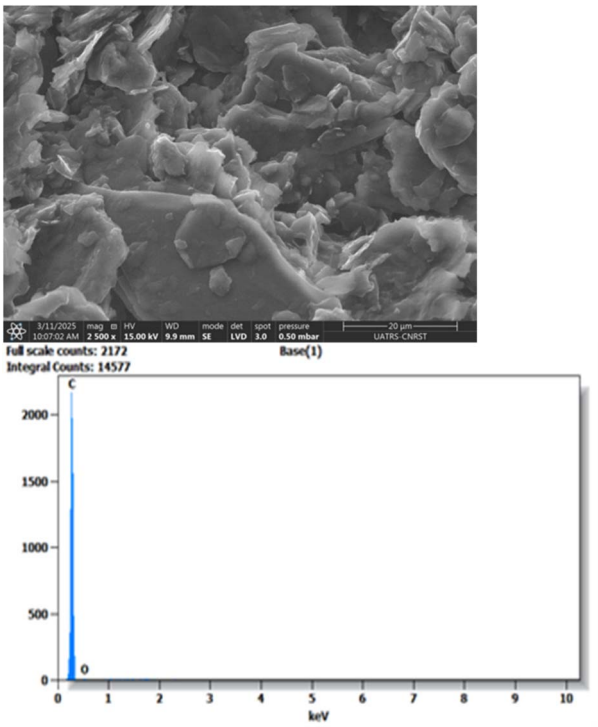

Fig. 3 SEM coupled with EDX analysis of CPE.

electrode, and a saturated calomel electrode (SCE) as the reference. Cyclic voltammetry (CV) was performed to detect pure totarolone in a 0.1 M NaCl supporting electrolyte (pH 4.5) at a concentration of 2 mM and a potential range from 1 V to 1 V

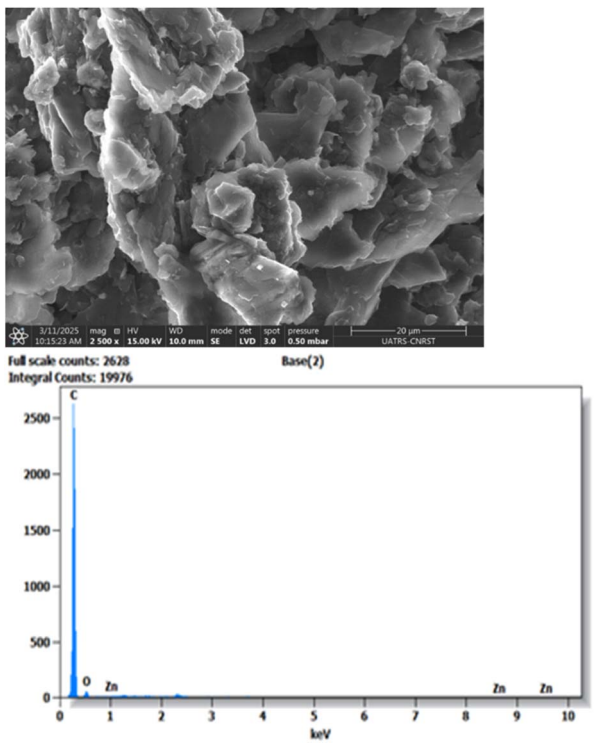

Fig. 4 SEM coupled with EDX analysis of bio-NPs-ZnO/CPE.

at a rate of 100 mV s^{-1}. Square-wave voltammetry (SWV) was performed for the direct detection of totarolone in 1 g of plant extract dissolved in 25 mL of 0.1 M NaCl solution, using a potential window from −1.5 V to 1.5 V with a step potential of 5 mV and an amplitude of 25 mV.

3. Results and discussion

3.1. Characterization of ZnO-NP synthesis

The FTIR analysis of the plant extract (Fig. 1A) reveals characteristic absorption bands of bioactive organic compounds at 3273, 2922, 1670, 1361, 1027, and 924 cm^{-1}, corresponding to O–H stretching of phenolic compounds, C–H vibrations,[28] C═C stretching of an alkene,[29] C═O stretching in polyphenol,[30] C–N stretching,[29] and out-of-plane ═C–H deformations, respectively. Upon bio-synthesis of ZnO nanoparticles (Fig. 1B), significant spectral changes occur, including the appearance of characteristic ZnO absorption peaks at 616 and 505 cm^{-1}, confirming successful nanoparticle formation.[31] Additionally, new bands emerge at 2171 cm^{-1} (C≡C stretching) and 1529 cm^{-1} (C═O vibrations),[32] while several bands shift to different frequencies, indicating direct interactions between plant metabolites and zinc ions. These spectral changes indicate that the plant extract components act as both reducing and stabilizing agents for Zn^{2+} ions, leading to the formation of bio-ZnO nanoparticles.

The XRD pattern shown in Fig. 2 confirms the crystalline nature of the bio-ZnO nanoparticles. The diffraction peaks observed at 2θ values of 31.0°, 34.4°, 36.1°, 47.0°, 56.0°, 63.0°, and 69.0° are indexed to the (100), (002), (101), (102), (110), (103), and (201) planes, respectively, which are characteristic of the hexagonal wurtzite structure of ZnO (JCPDS card no. 01-076-0704). Furthermore, the average crystallite size, calculated using the Scherrer equation ($D = K\lambda/\beta\cos\theta$),[33] was found to be approximately 10 nm, demonstrating the nanoscale dimension of the obtained ZnO particles. These results are consistent with previous literature reports.[34–36]

SEM images reveal that the bare CPE surface (Fig. 3) exhibits a relatively smooth yet irregular morphology with minimal aggregation. In contrast, the ZnO-modified CPE (Fig. 4) displays a more porous, heterogeneous surface, composed of highly irregular particles with a pronounced tendency to aggregate. These morphological features are consistent with previous literature reports.[37,38] The successful incorporation of ZnO is further confirmed by the detection of Zn and O peaks in the EDX spectra. After 20 minutes of preconcentration in a 2 mM totarolone solution (Fig. 5), the ZnO-modified electrode surface shows notable densification and smoothing, along with the formation of small clusters, likely corresponding to ZnO–totarolone complexes. These clusters are clearly distinct from those observed on the bare CPE and the ZnO-modified CPE (Fig. 4), confirming the effective interaction between totarolone and the ZnO-modified electrode.[39]

3.2. Electrochemical behavior of totarolone on the CPE and bio-NPs-ZnO/CPE

Electrochemical interaction between totarolone and ZnO NPs in 0.1 M NaCl solution was studied by CV. Fig. 6 shows CV of the

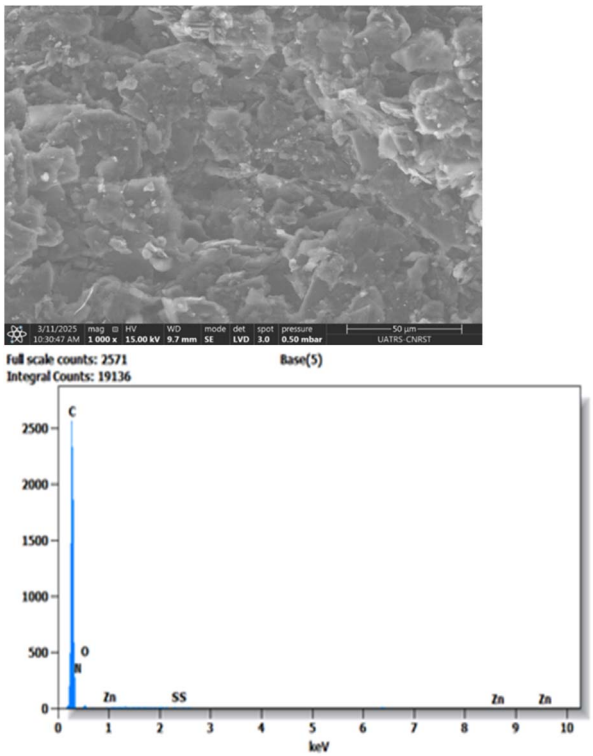

Fig. 5 SEM coupled with EDX analysis of bio-NPs-ZnO/CPE after 20 min of preconcentration in 2 mM of totarolone.

CPE and bio-NPs-ZnO/CPE with 2 mmol L^{-1} of totarolone at a scan rate of 100 mV s^{-1} in a potential range of −1.0 to +1.0 V. While the CPE shows only a very small oxidation peak, a significantly larger oxidation peak is observed at 231.52 μA for bio-NPs-ZnO/CPE. This enhancement indicates the superior electrochemical performance of the modified electrode, which can be attributed to the increased number of active sites on its surface. These sites facilitate greater accessibility and adsorption of totarolone, likely due to the expanded internal surface area of the nanomaterial. Consequently, the bio-NPs-ZnO/CPE

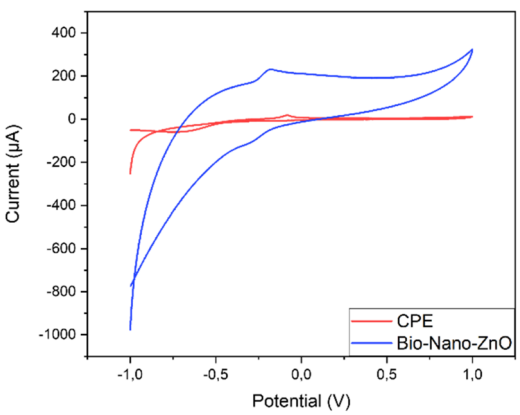

Fig. 6 CV measurements for both the CPE and bio-NPs-ZnO/CPE in 2 mM totarolone dissolved in 0.1 M NaCl, at a scan rate of 100 mV s^{-1} and a start potential of −1.0 V *vs.* Hg/Hg_2Cl_2, KClsat.

demonstrates strong potential as a sensitive electrochemical sensor for totarolone detection.[40]

3.3. Optimization of experimental variable

3.3.1. Scan rate. To analyze the reaction kinetics of totarolone at the modified CPE, the effect of the scan rate (50–250 mV s^{-1}) on the oxidation peak current (I_{pa}) was investigated. As shown in Fig. 7A, I_{pa} increased steadily with increasing scan rate. Fig. 7B shows that the curve of the scan rate *vs.* anodic current was more linear than the plot of the square root of the scan rate *vs.* the anodic current (Fig. 7C), revealing that mass transfer of totarolone on the bio-ZnO/CPE surface was mainly controlled by adsorption instead of diffusion.[41,42]

3.3.2. pH effect. The influence of pH on the electrode response was investigated over a pH range from 3.5 to 6.5. The pH-dependent behavior (Fig. 8A) can be rationalized by a balance between adsorption and electron-transfer kinetics. From pH 3.5 to 4.5, hydrogen bonding between totarolone and hydroxylated bio-ZnO enhances adsorption, increasing the peak current. At pH 5.5, partial deprotonation to phenolate reduces hydrogen bonding and introduces electrostatic repulsion with the bio-ZnO surface, leading to a transient decrease. At pH 6.5, the predominance of the phenolate form of totarolone—more electroactive—improves electron-transfer kinetics enough to overcome the reduced adsorption, resulting in a slightly higher current.[43]

Furthermore, information regarding the number of proton(s) and electron(s) involved in the redox process can be used to determine the structural evolution of totarolone after the electrooxidation reaction on bio-ZnO-NPs/CPE using eqn (1):[44]

$$E_p = -2.303\frac{mRT}{nF}\mathrm{pH} \quad (1)$$

where E_p is the redox potential (mV), R is the gas constant (J mol^{-1} K^{-1}), T is the temperature (K), F is the Faraday constant

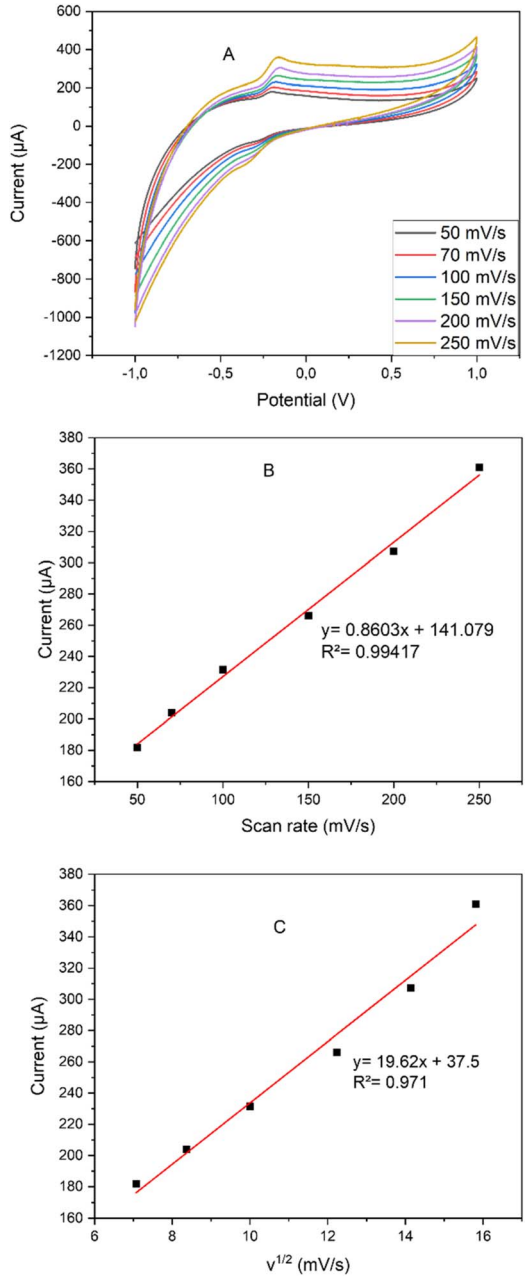

Fig. 7 (A) Bio-NPs-ZnO/CPE CVs in 0.1 M NaCl solution (pH = 4.5) with 2 mM of totarolone at various SRs and a start potential of −1.0 V *vs.* Hg/Hg_2Cl_2, KClsat. (B) Plot of I_{pa} *versus* v. (C) Plot of I_{pa} *versus* $v^{1/2}$.

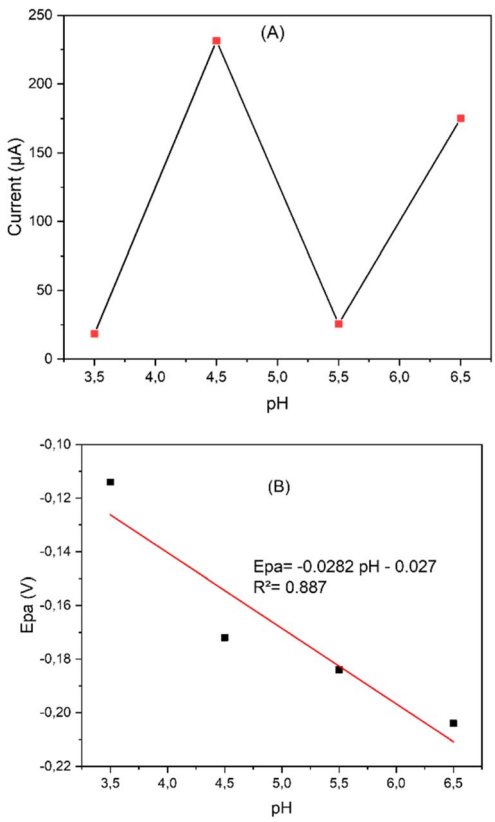

Fig. 8 (A) Influence of solution pH on the oxidation peak current of totarolone recorded at bio-NPs-ZnO/CPE in 0.1 M NaCl, at a scan rate of 100 mV s^{-1} and a start potential of −1.0 V *vs.* Hg/Hg_2Cl_2, KClsat, and (B) linear plot of E_{pa} *vs.* pH.

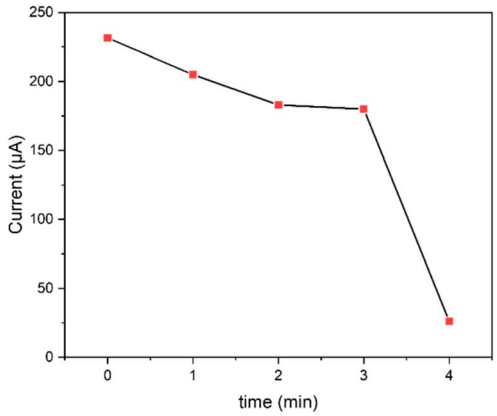

Fig. 9 Effect of accumulation time on the peak current of totarolone at the bio-NPs-ZnO/CPE electrode in 0.1 M NaCl solution (pH 4.5), at a scan rate of 100 mV s^{-1} and a start potential of −1.0 V *vs.* Hg/Hg_2Cl_2, KClsat.

(C mol^{-1}), and m/n is the slope, which represents the ratio of proton(s) and electron(s). The slope of the corresponding linear plot of E_{pa} *vs.* pH (Fig. 8B) is 28.2 mV pH^{-1}, which is close to the theoretical Nernstian value (29.50 mV) for a two-electron and one-proton transfer redox process.[45,46] Therefore, a plausible redox reaction for totarolone oxidation can be proposed as

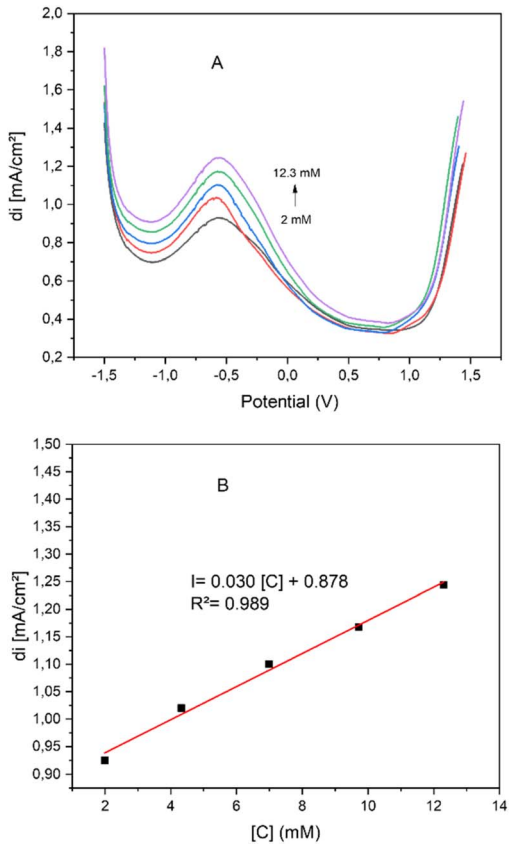

Fig. 10 (A) SW voltammograms of bio-NPs-ZnO/CPE for the determination of totarolone in 0.1 M NaCl solution (pH 4.5); amplitude: 20 mV; potential step: 5 mV; start potential: −1.5 V *vs.* Hg/Hg_2Cl_2, KClsat. (B) Calibration graph corresponding to the peak of totarolone obtained from various concentrations in the range of 2 to 12.3 mM.

$$\text{Totarolone–(OH)}_n \text{ (adsorbed on ZnO)} \rightarrow \text{Totarolone–(O}^{ox})_n + nH^+ + 2ne^- \quad (2)$$

3.3.3. Accumulation time effect. The effect of accumulation time (AT) on the detection of totarolone was investigated over a range of 0 to 4 minutes in a 0.1 M NaCl solution (pH 4.5) containing 2 mM totarolone. As shown in Fig. 9, the peak current decreased with increasing accumulation time, indicating that the modified electrode enables rapid detection of totarolone.[47] The decrease in the oxidation peak current observed with increasing accumulation time can be explained by the saturation of active sites on the surface of bio-ZnO/CPE. During the accumulation step, a negative potential of −0.4 V was applied, which promotes the adsorption of totarolone onto the ZnO-modified electrode surface. Initially, the adsorption is rapid, leading to a measurable current increase; however, as the accumulation time extends, the electrode surface becomes progressively saturated. This saturation reduces the availability of free active sites for further electron transfer, resulting in a gradual decrease of the oxidation peak current over time.[48]

Fig. 5 provides complementary evidence for this behavior. After 20 minutes of preconcentration, the SEM image shows the formation of small clusters on the bio-ZnO/CPE surface. These clusters correspond to complexes formed between bio-ZnO and totarolone. The presence of these clusters supports the notion that the decrease in current with longer accumulation times arises from the formation of an adsorbed layer, which limits the electron transfer efficiency.

3.3.4. Concentration effect. The SWV voltammograms at different totarolone concentrations (Fig. 10A) show that the current intensity increased with the increase of the concentration. This demonstrates the linear relationship (R^2 = 0.989) from 2 mM to 12.3 mM illustrated in Fig. 10B. The sensor's sensitivity was validated by the calculation of the detection limit (LOD = $3S_b/S$) and the quantification limit (LOQ = $10S_b/S$). S_b is the standard deviation of seven measurements and S is the slope of the calibration plot.[49,50] The findings obtained are illustrated in Table 1.

A calibration curve equation (I = 0.03 [C] + 0.878) was obtained from the standard curve of current as a function of concentration. This equation is then used to quantify totarolone in the extract.

3.3.5. Quantification of totarolone in the extract. To quantify the concentration of totarolone in the extract, a solution was prepared by dissolving 1 g of the extract in 25 mL of a 0.1 M NaCl solution, ensuring optimal solubilization of totarolone. The analysis was performed using square wave voltammetry (SWV) over a potential range from −1.5 V to 1.5 V. Fig. 11 shows

Table 1 LOD and LOQ values for totarolone at bio-NPs-ZnO/CPE

Concentration range	LOD	LOQ
2–12.3 mM	1.19 μM	3.98 μM

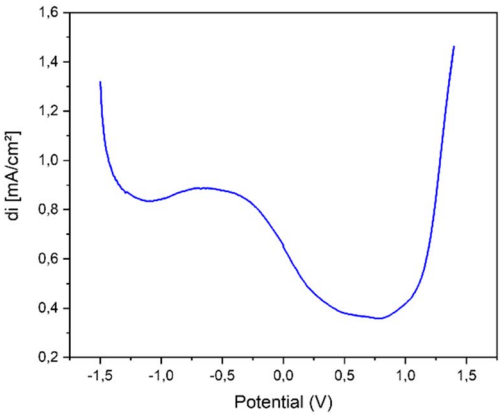

Fig. 11 SW voltammograms of bio-NPs-ZnO/CPE for the quantification of the totarolone in 1 g of extract dissolved in 25 mL of 0.1 M NaCl solution; amplitude: 20 mV; potential step: 5 mV; start potential: −1.5 V *vs.* Hg/Hg_2Cl_2, KClsat.

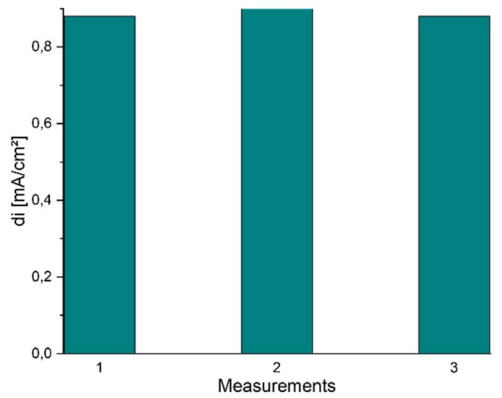

Fig. 12 Evaluation of the reproducibility of bio-NPs-ZnO/CPE; amplitude: 20 mV; potential step: 5 mV; start potential: −1.5 V *vs.* Hg/Hg_2Cl_2, KClsat.

a current peak of 0.882 mA at a potential of −0.5 V, attributed to totarolone, confirming its presence in the sample. Using the previously obtained calibration curve equation, the concentration of totarolone in 1 g of extract was determined to be 0.133 mM. This value provides an estimate of totarolone's content in the extract and helps assess the efficiency of the extraction process.

3.3.6. Reproducibility. To evaluate the repeatability of bio-ZnO-NPs/CPE in the quantification of totarolone, three consecutive measurements were performed. As shown in Fig. 12, the results demonstrate consistent sensor performance, confirming the method's reliability and reproducibility in detecting the molecule within the extract solution.[51]

3.3.7. Stability. The stability of bio-NPs-ZnO/CPE was evaluated after two months of storage. The electrode retained approximately 98% of its original response, as shown in Fig. 13, demonstrating its excellent long-term stability for the quantification of totarolone.

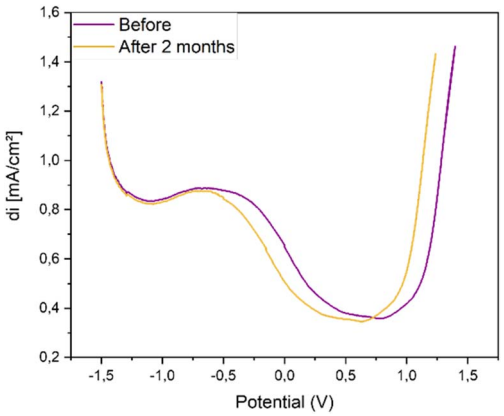

Fig. 13 Bio-NPs-ZnO/CPE stability; amplitude: 20 mV; potential step: 5 mV; start potential: −1.5 V *vs.* Hg/Hg_2Cl_2, KClsat.

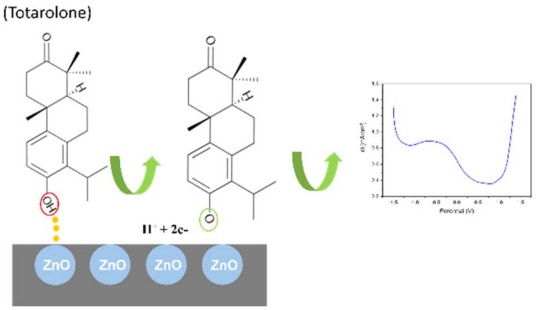

Fig. 14 Proposed mechanism of totarolone detection on bio-NPs-ZnO/CPE.

3.4. Proposed electrochemical sensing mechanism

The surface of biosynthesized ZnO (Fig. 14), enriched with hydroxyl groups (OH), along with residual organic groups from the plant extract (C═O, C═C, and C–N), provides abundant active sites for the adsorption of totarolone. The molecule interacts primarily *via* hydrogen bonding with the hydroxyl groups of ZnO, while the residual organic groups contribute secondary polar interactions, stabilizing the molecule on the surface. This adsorption facilitates a proton-coupled electron-transfer (PCET) process, allowing efficient transfer of electrons from totarolone to the electrode. The ZnO nanoparticles not only provide a high surface area for adsorption but also promote electron transfer between totarolone and the electrode surface, thereby enhancing the oxidation current. This mechanism explains the well-defined anodic peak observed during voltammetric measurements.

4. Conclusions

This study reports the first quantification of totarolone using bio-ZnO nanoparticles synthesized *via Calamintha nepeta* extract. FTIR analyses confirmed the successful formation of ZnO nanoparticles, while XRD revealed a hexagonal wurtzite structure with an average crystallite size of ∼10 nm. SEM-EDX validated the incorporation of ZnO into the CPE matrix and

demonstrated effective interactions with totarolone. CV indicated that the electrochemical process of totarolone on the bio-ZnO/CPE surface is adsorption-controlled, involving a two-electron/one-proton transfer. The sensor exhibited high sensitivity, a low detection limit (1.19 μM), and excellent stability and reproducibility. Finally, the totarolone content in 1 g of extract was determined to be 0.133 mM. These findings highlight the potential of green nanotechnology to advance analytical platforms for natural product research and open new avenues for environmentally responsible applications in pharmacology and the food industry.

Author contributions

This study was conducted with significant contributions from all authors. Omar Anor and Sofia Kerouad conceptualized the study and designed and executed the experimental work. Wissal Kotmani prepared the samples. Issam Forsal supervised the research. Mustapha Bouzaid and Latifa Bouissane reviewed the manuscript structure. All authors have reviewed and approved the final manuscript for submission.

Conflicts of interest

There are no conflicts to declare.

Abbreviations

CPE	Carbon paste electrode
CV	Cyclic voltammetry
CVs	Cyclic voltammograms
LOD	Detection limit
LOQ	Quantification limit
NPs	Nanoparticles
SRs	Scan rates
SW	Square wave
SWV	Square wave voltammetry

Data availability

All data supporting the findings of this study are contained within the main manuscript.

References

1 A. Kalyniukova, J. Holuša, D. Musiolek, J. Sedlakova-Kadukova, J. Płotka-Wasylka and V. Andruch, *Ind. Crop. Prod.*, 2021, **172**, 114047, DOI: **10.1016/j.indcrop.2021.114047**.
2 L. Grigore-Gurgu, L. Dumitrașcu and I. Aprodu, *Molecules*, 2025, **30**(6), 1304, DOI: **10.3390/molecules30061304**.
3 A. Ayed, L. Caputo, V. De Feo, F. Nazzaro, F. Fratianni, I. Amri, L. Hamrouni, Y. Mabrouk and F. Polito, *Chem. Biodiversity*, 2024, **22**(1), e202401618, DOI: **10.1002/cbdv.202401618**.
4 S. Khatib, O. Nerya, R. Musa, M. Shmuel and S. Tamir, *Bioorg. Med. Chem.*, 2005, **13**, 433–441, DOI: **10.1016/j.bmc.2004.10.010**.
5 W. Rached, F. Z. Zeghada, M. Bennaceur, L. Barros, R. C. Calhelha, S. Heleno, M. J. Alves, A. M. Carvalho and A. Marouf, *Ind. Crops Prod.*, 2018, **112**, 460–466, DOI: **10.1016/j.indcrop.2017.12.037**.
6 M. Saber, H. Harhar, L. El Hattabi, G. Zengin, A. Bouyahya and M. Tabyaoui, *Int. J. Second. Metab.*, 2021, **8**, 352–363, DOI: **10.21448/ijsm.989436**.
7 Y. O. Nuñez, I. S. Salabarria, I. G. Collado and R. Hernández-Galán, *J. Agric. Food Chem.*, 2006, **54**, 7517–7521, DOI: **10.1021/jf061436m**.
8 H. C. Wu, L. L. Shiu, S. W. Wang, C. Y. Huang, T. H. Lee, P. J. Sung and Y. H. Kuo, *Plants*, 2023, **12**, 3828, DOI: **10.3390/plants12223828**.
9 M. Yabré, L. Ferey, I. T. Somé and K. Gaudin, *Molecules*, 2018, **2**(5), 065, DOI: **10.3390/molecules23051065**.
10 M. Mesud Hurkul, A. Cetinkaya, S. Yayla and S. A. Ozkan, *J. Chromatogr. Open*, 2024, **5**, 100131, DOI: **10.1016/j.jcoa.2024.100131**.
11 C. Berkel and O. Özbek, *Electroanalysis*, 2024, **36**(11), e202400286, DOI: **10.1002/elan.202400286**.
12 P. K. Kalambate, Z. Rao, Dhanjai, J. Wu, Y. Shen, R. Boddula and Y. Huang, *Biosens. Bioelectron.*, 2020, **163**, 112270, DOI: **10.1016/j.bios.2020.112270**.
13 F. Tulli, M. Lemos, D. Gutiérrez, S. Rodríguez, B. A. L. de Mishima and V. I. P. Zanini, *Food Technol. Biotechnol.*, 2020, **58**(2), 183–191, DOI: **10.17113/ftb.58.02.20.6593**.
14 A. Curulli, *Molecules*, 2020, **25**(23), 5759, DOI: **10.3390/molecules25235759**.
15 A. Afkhami, F. Kafrashi and T. Madrakian, *Ionics*, 2015, **21**(10), 1–11, DOI: **10.1007/s11581-015-1486-z**.
16 L. Luo, D. Li, J. Zang, C. Chen, J. Zhu, H. Qiao, Y. Cai, K. Lu, X. Zhang and Q. Wei, *Energy Technol.*, 2017, **5**, 1364–1372, DOI: **10.1002/ente.201600686**.
17 M. Rafique, R. Tahir, S. S. A. Gillani, M. Bilal Tahir, M. Shakil, T. Iqbal and M. O. Abdellahi, *Int. J. Environ. Anal. Chem.*, 2020, **102**, 23–38, DOI: **10.1080/03067319.2020.1715379**.
18 N. S. Powar, V. Patel, P. Pagare and R. Pandav, *Chem. Methodol.*, 2019, **3**, 457–480, DOI: **10.22034/chemm.2019.154075.1112**.
19 M. A. El-Hashemy and A. Sallam, *J. Mater. Res. Technol.*, 2020, **9**, 13509, DOI: **10.1016/j.jmrt.2020.09.078**.
20 K. Prabakaran, G. Shanmugavel and I. J. Pharmacogn, *Phytochem.*, 2017, **9**, 985–989, DOI: **10.25258/phyto.v9i07.11168**.
21 S. Kerouad, I. Forsal and S. Lahmady, *Curr. Top. Electrochem.*, 2023, **24**, 123–131.
22 S. Aronbaev, D. Aronbaev and D. Isakova, *BIO Web Conf.*, 2024, **116**, 06002, DOI: **10.1051/bioconf/202411606002**.
23 W. Bouali, N. Erk and A. Ayse Genc, *Anal. Methods*, 2024, **16**(11), 1623–1630, DOI: **10.1039/D3AY02194G**.
24 United Nations, *Transforming our world: The 2030 agenda for sustainable development*, 2015.
25 S. Raut, Dr. P. V. Thorat and R. Thakre, *Int. J. Sci. Res.*, 2015, **4**(5), 1225–1228, DOI: **10.21275/SUB154428**.
26 T. Madrakian, H. Ghasemi, E. Haghshenas and A. Afkhami, *RSC Adv.*, 2016, **6**, 33851–33856, DOI: **10.1039/C6RA03666J**.

27 L. Moujir, A. Seca, A. Silva and M. Barreto, *Planta Med.*, 2008, **74**, 751–753, DOI: **10.1055/s-2008-1074529**.
28 N. Kumar, G. Irfan, Udayabhanu and G. Nagaraju, *Mater. Today Proc.*, 2021, **8**(5), 3116–3124, DOI: **10.1016/j.matpr.2020.09.494**.
29 K. Dulta, G. Koşarsoy Ağçeli, P. Chauhan, R. Jasrotia and P. K. Chauhan, *J. Cluster Sci.*, 2022, **33**, 603–617, DOI: **10.1007/s10876-020-01962-w**.
30 W. Muhammad, N. Ullah, M. Haroon and B. H. Abbasi, *RSC Adv.*, 2019, **9**, 29541, DOI: **10.1039/C9RA04424H**.
31 C. W. Wong, Y. San, S. Chan, J. Jeevanandam and K. Pal, *J. Cluster Sci.*, 2020, **31**, 367–389, DOI: **10.1007/s10876-019-01651-3**.
32 R. Dobrucka, *Iran. J. Sci. Technol. Trans. A-Science*, 2018, **42**, 547–555, DOI: **10.1007/s40995-016-0076-x**.
33 M. A. Edaala, K. Belkodia, E. M. El Mouchtari, A. Alaoui Tahiri, S. Rossignol, S. Lebarillier, A. Piram, P. Wong-Wah-Chung, M. A. Maher and S. Rafqah, *J. Water Proc. Eng.*, 2025, **70**, 107098, DOI: **10.1016/j.jwpe.2025.107098**.
34 H. Hameed, A. Waheed, M. S. Sharif, M. Saleem, A. Afreen, M. Tariq, A. Kamal, W. A. Al-Onazi, D. A. Al Farraj, S. Ahmad and R. M. Mahmoud, *Micromachines*, 2023, **14**(5), 928, DOI: **10.3390/mi14050928**.
35 A. S. Abdelbaky, T. A. Abd El-Mageed, A. O. Babalghith, S. Selim and A. M. H. A. Mohamed, *Antioxidants*, 2022, **11**(8), 1444, DOI: **10.3390/antiox11081444**.
36 X. T. Tran, T. T. L. Bien, T. V. Tran and T. T. T. Nguyen, *Nanoscale Adv.*, 2024, **6**(19), 4885–4899, DOI: **10.1039/d4na00326h**.
37 Y. Ya. C. Jiang, T. Li, J. Liao, Y. Fan, Y. Wei, F. Yan and L. Xie, *Chem. Sensors*, 2017, **17**, 545, DOI: **10.3390/s17030545**.
38 G. Karim-Nezhad, Z. Khorablou, M. Zamani, P. Seyed Dorraji and M. Alamgholiloo, *J. Food Drug Anal.*, 2016, **8**((2)), 293–301, DOI: **10.1016/j.jfda.2016.10.002**.
39 C. Laghlimi, Y. Ziat, A. Moutcine, M. Hammi, Z. Zarhri, R. Maallah, O. Ifguis and A. Chtaini, *Chem. Data Collect.*, 2020, **29**, 100496, DOI: **10.1016/j.cdc.2020.100496**.
40 S. Kerouad, I. Forsal, A. Talfana, M. Kasbaji and M. A. Edaala, *Inorg. Chem. Commun.*, 2025, **177**, 114232, DOI: **10.1016/j.inoche.2025.114232**.
41 Y. Feye, A. Diro, G. Sisay and S. A. Kitte, *Sci. Afr.*, 2023, **22**, e01909, DOI: **10.1016/j.sciaf.2023.e01909**.
42 N. Elgrishi, K. J. Rountree, B. D. McCarthy, E. S. Rountree, T. T. Eisenhart and J. L. Dempsey, *J. Chem. Educ.*, 2018, **6**, 197–206, DOI: **10.1021/acs.jchemed.7b00361**.
43 M. Sjödin, J. Hjelm, A. William Rutherford and R. Forster, *J. Electroanal. Chem.*, 2020, **859**, 113856, DOI: **10.1016/j.jelechem.2020.113856**.
44 T. Imtiaz, A. Shah, N. Ullah, F. J. Iftikhar, I. Shah, S. M. Shah and S. S. Shah, *Water*, 2022, **5**, 1–13, DOI: **10.1038/s41545-022-00213-x**.
45 W. P. Wicaksono, H. Dang, S. Lee and J. Choo, *Appl. Surf. Sci.*, 2024, **649**, 159163, DOI: **10.1016/j.apsusc.2023.159163**.
46 C. Laghlimi, A. Moutcine, A. Chtaini, J. Isaad, A. Soufi, Y. Ziat, H. Amhamdi and H. Belkhanchi, *ADMET & DMPK*, 2023, **11**(2), 151–173, DOI: **10.5599/admet.1709**.
47 R. L. Zamboni, C. Kalinke, L. M. C. Ferreira, M. A. P. Papi, E. S. Orth and C. E. Banks, *Anal. Methods*, 2025, **17**(9), 2214–2223, DOI: **10.1039/d4ay02240h**.
48 A. Moutcine, C. Laghlimi, Y. Ziat Y, M. A. Smaini, S. El Qouatli, M. Hammi and A. Chtaini, *Inorg. Chem. Commun.*, 2020, **116**, 107911, DOI: **10.1016/j.inoche.2020.107911**.
49 E. B. Kim, M. Imran, E. H. Lee, M. Shaheer Akhtar and S. Ameen, *Chemosphere*, 2022, **286**, 131695, DOI: **10.1016/j.chemosphere.2021.131695**.
50 G. Li, S. Feng, L. Yan, L. Yang, B. Huo, L. Wang, S. Luo and D. Yang, *Food Chem.*, 2023, **404**, 134609, DOI: **10.1016/j.foodchem.2022.134609**.
51 N. An, N. Su, X. R. Li, J. Y. Liu and Q. Y. Wang, *J. Electrochem.*, 2025, **31**(3), 2407241, DOI: **10.61558/2993-074X.3503**.